AEM
Journals.ASM.org

Decreased Xylitol Formation during Xylose Fermentation in *Saccharomyces cerevisiae* Due to Overexpression of Water-Forming NADH Oxidase

Guo-Chang Zhang, Jing-Jing Liu, and Wen-Tao Ding

Department of Biochemical Engineering, School of Chemical Engineering and Technology, Tianjin University, Tianjin, China

The recombinant xylose-fermenting *Saccharomyces cerevisiae* strain harboring xylose reductase (XR) and xylitol dehydrogenase (XDH) from *Scheffersomyces stipitis* requires NADPH and NAD^+, creates cofactor imbalance, and causes xylitol accumulation during growth on D-xylose. To solve this problem, *noxE*, encoding a water-forming NADH oxidase from *Lactococcus lactis* driven by the *PGK1* promoter, was introduced into the xylose-utilizing yeast strain KAM-3X. A cofactor microcycle was set up between the utilization of NAD^+ by XDH and the formation of NAD^+ by water-forming NADH oxidase. Overexpression of *noxE* significantly decreased xylitol formation and increased final ethanol production during xylose fermentation. Under xylose fermentation conditions with an initial D-xylose concentration of 50 g/liter, the xylitol yields for of KAM-3X(pPGK1-noxE) and control strain KAM-3X were 0.058 g/g xylose and 0.191 g/g, respectively, which showed a 69.63% decrease owing to *noxE* overexpression; the ethanol yields were 0.294 g/g for KAM-3X(pPGK1-noxE) and 0.211 g/g for the control strain KAM-3X, which indicated a 39.33% increase due to *noxE* overexpression. At the same time, the glycerol yield also was reduced by 53.85% on account of the decrease in the NADH pool caused by overexpression of *noxE*.

Bioethanol production from lignocellulosic feedstock has received considerable attention in recent years due to the abundance and low cost of the feedstock compared to those starch- and sucrose-based materials. *Saccharomyces cerevisiae*, which has been used traditionally and remains the organism of choice for industrial bioethanol production from hexose, does not naturally utilize D-xylose, the second major constituent of the hydrolysate of lignocellulosic biomass (26).

A lot of research has been done during the last 20 years on the yeast conversion of D-xylose to ethanol, with major efforts focused on the functional expression of bacterial and fungal xylose-utilizing genes and manipulating the pentose phosphate pathway (PPP) to enhance D-xylose utilization and fermentation in *S. cerevisiae* (7, 8, 14, 16, 17). There have been two common metabolic pathways for D-xylose utilization in fungi and bacteria. In most fungi and xylose-fermenting yeasts, such as *Scheffersomyces stipitis* (formerly known as *Pichia stipitis*) (20), *Candida shehatae*, and *Pachysolen tannophilus*, D-xylose first is reduced to xylitol by NAD(P)H-dependent xylose reductase (XR), which is encoded by *XYL1*, and then xylitol is oxidized to D-xylulose by NAD^+-dependent xylitol dehydrogenase (XDH), which is encoded by *XYL2* (26, 30, 37). Finally, D-xylulose is phosphorylated into xylulose-5-phosphate, which is further metabolized through the PPP (31). An alternative pathway is the non-cofactor-requiring xylose isomerase (XI) pathway from bacteria or fungi, which can isomerize D-xylose to D-xylulose (9, 21).

Introducing the *Scheffersomyces stipitis* XR-XDH system into *S. cerevisiae* has successfully allowed D-xylose to be fermented to ethanol. However, a major drawback of the XR-XDH system is cofactor imbalance, because XR strongly prefers NADPH over NADH (35) and XDH uses NAD^+ (14) as a cofactor. This cofactor imbalance leads to the excess accumulation of xylitol and reduced final ethanol yield. The surplus NADH cannot be reoxidized sufficiently through respiration under oxygen-limited conditions during bioethanol fermentation and thus causes the formation of by-product glycerol (1, 26), which further affects ethanol yield. To overcome this problem, the XI pathway has been introduced into *S. cerevisiae*, resulting in higher ethanol yield but lower growth rate and ethanol productivity during xylose fermentation (2, 18, 21, 25). Several metabolic engineering approaches have been implemented previously to balance the cofactors in *S. cerevisiae*: shifting ammonia assimilation from being NADPH to NADH dependent by the deletion of *gdh1* and the overexpression of *GDH2* (6); the overexpression of the *Kluyveromyces lactis GDP1* gene, which encodes an $NADP^+$-dependent glyceraldehyde-3-phosphate dehydrogenase (GAPDH) (36); the expression of the *gapN* gene, which encodes a nonphosphorylating $NADP^+$-dependent GAPDH from *Streptococcus* mutants (3); the overexpression of NADH kinase, which is encoded by the *POS5* gene (13); etc. Another promising approach for reducing xylitol production and enhancing ethanol yield using recombinant *S. cerevisiae* involves alterations in the coenzyme specificity of XR (changing the preference of NADPH to NADH) (15, 22, 32, 38, 40) or XDH (with the coenzyme preference shifted from NAD^+ to $NADP^+$) (12, 27, 39) by protein engineering.

Recently, the water-forming (nontoxic to yeast) NADH oxidase encoded by *noxE* from *Lactococcus lactis* was studied in *S. cerevisiae* (10, 11, 34). This NADH oxidase specifically uses NADH and provides an extra route for the oxidation of this reduced nucleotide, accompanied by deoxidizing O_2 to H_2O, when oxygen is available (24). The NADH oxidase, predominantly localized in the

Received 23 August 2011 **Accepted** 28 November 2011
Published ahead of print 9 December 2011
Address correspondence to J.-J. Liu, liujingjing@tju.edu.cn.
G.-C.Z. and J.-J.L. contributed equally to this work.

doi:10.1128/AEM.06635-11

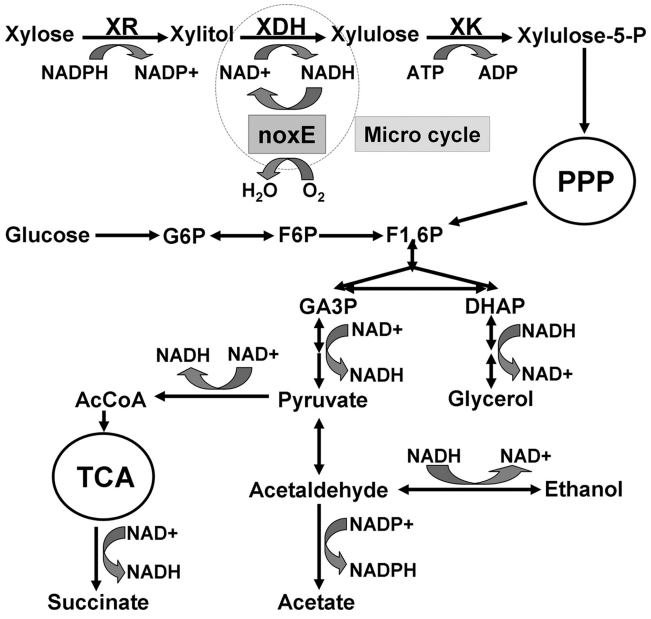

FIG 1 Glucose and xylose metabolism pathway in recombinant *Saccharomyces cerevisiae*. The key enzymes and the cofactor requirements that were identified in the central metabolism are shown. Abbreviations: XR, xylose reductase; XDH, xylitol dehydrogenase; XK, xylulokinase; G6P, glucose-6-phosphate; F6P, fructose-6-phosphate; F1,6P, fructose-1,6-bisphosphate; PPP, pentose phosphate pathway; GA3P, glyceraldehyde-3-phosphate; DHAP, dihydroxyacetone phosphate; AcCoA, acetylcoenzyme A; TCA, tricarboxylic acid cycle.

cytosol in *S. cerevisiae*, has a high affinity for NADH and is capable of replacing the function of native NADH dehydrogenases encoded by *NDE1* and *NDE2* (34). As described previously, xylitol is oxidized to D-xylulose by NAD^+-dependent XDH, leading to excess NADH and insufficient NAD^+, which in turn gives rise to the accumulation of xylitol. Based on this background, we envisage that the expression of water-forming NADH oxidase in a xylose-utilizing yeast strain is able to form a microcycle between NADH and NAD^+ and can solve this cofactor imbalance problem (Fig. 1). Results in this study showed that the xylitol yield was reduced and the corresponding ethanol yield was increased after introducing the *noxE* gene into our xylose-utilizing yeast strain KAM-3X.

MATERIALS AND METHODS

Strains, media, and growth conditions. *Escherichia coli* Top10 was used for plasmid construction and propagation. *E. coli* was grown in LB medium (5 g/liter yeast extract, 10 g/liter tryptone, 10 g/liter NaCl, pH 7.0) at 37°C, and ampicillin (50 μg/ml) was added when required. The *noxE* gene, encoding a water-forming NADH oxidase, was from *Lactococcus lactis*, which also was grown in LB medium. The yeast strain used in this study was KAM-2 (23), which was derived from the diploid industrial strain TH-AADY (Angel Yeast Co., Ltd., China). Yeast strains were grown in yeast extract-peptone-dextrose (YPD) medium (10 g/liter yeast extract, 20 g/liter peptone, and 20 g/liter glucose) or defined mineral medium (YSCD) containing 6.7 g/liter yeast nitrogen base without amino acids and supplemented with the appropriate auxotrophic requirements and 20 g/liter glucose at 30°C. A 5-fluoroorotic acid (5-FOA) plate was used for the counterselection of the URA3 gene. Xylose fermentation was performed at 30°C in a medium containing 6.7 g/liter yeast nitrogen base without amino acids and supplemented with the appropriate auxotrophic requirements and 50 g/liter D-xylose (YSCX medium).

DNA manipulation and plasmid and strain construction. The plasmid pTPI1-XKS1, used for the overexpression of *XKS1* driven by the *TPI1* promoter, was constructed as follows. First, the PCR fragment amplified using primer pair pXKS1-U and pXKS1-D (Table 1) was double digested with EcoRI and KpnI and ligated to YIplac211 digested with the same enzyme pair, resulting in plasmid YIplac211-pXKS1. Second, the *TPI1* promoter was amplified from yeast genomic DNA using primer pair pTPI1-U and pTPI1-D (Table 1), carrying KpnI and BamHI restriction sites, respectively. The PCR product was digested by KpnI-BamHI and inserted into YIplac211-pXKS1 digested with the same enzyme pair, generating plasmid YIplac211-pXKS1-pTPI1. Finally, the open reading frame (ORF) of *XKS1* was amplified using primer pair XKS1-U and XKS1-D (Table 1) containing BamHI and PstI, respectively. The PCR product was double digested with BamHI-PstI and ligated with YIplac211-pXKS1-pTPI1, which was digested with the same enzyme pair, to construct plasmid YIplac211-pXKS1-pTPI1-XKS1 (pTPI1-XKS1) (Table 2). The plasmid pTPI1-XKS1 was linearized with SacI and transformed into KAM-2 with the lithium acetate method for integration. A 5-FOA plate was used for the counterselection of the *URA3* gene. The correct integration was verified by analytical PCR using primer pair XKS1-CKU and XKS1-CKD (Table 1) and designated KAM-XKS1 (Table 3).

XYL1 and *XYL2* from *Scheffersomyces stipitis*, driven by the promoters *HXT7* and *FBA1*, respectively, were integrated into the yeast chromosome between *NRG1* and *HEM13* without disturbing the function of the two genes. The plasmid YIp-NH8 (Table 2), which was used for integration, was constructed as follows. (i) The first homologous fragment for integration, NH1, was amplified from yeast genomic DNA using primer pair NH-1U and NH-1D. The PCR fragment was double digested with EcoRI and KpnI and ligated with plasmid YIplac211 to construct YIp-NH1. (ii) The second homologous fragment, NH2, was amplified using primer pair NH-2U and NH-2D, containing the restriction sites for SphI and HindIII, respectively. The PCR product was double digested by SphI-HindIII and ligated to YIp-NH1 with the same enzyme pair, generating plasmid YIp-NH2. (iii) The promoter of *HXT7*, which was used for the strong expression of *XYL1*, was amplified using primer pair pHXT7-U, carrying KpnI, and pHXT7-D, carrying SmaI. The PCR product pHXT7 was double digested with KpnI-SmaI and ligated to YIp-NH2 to form plasmid YIp-NH3. (iv) *XYL1* from *Scheffersomyces stipitis* was amplified with primer pair XYL1-U, carrying SmaI, and XYL1-D, carrying XbaI-BamHI. The resulting PCR fragment was double digested with SmaI and XbaI and ligated to YIp-NH3 digested with the same enzyme pair, resulting in plasmid YIp-NH4. (v) The terminator of *HXT7* was amplified using primer pair tHXT7-U, carrying BamHI, and tHXT7-D, carrying SphI-NotI-XbaI. The resulting DNA fragment was digested by BamHI and SphI and ligated to YIp-NH4 digested with the same enzyme pair to generate YIp-NH5. (vi) The *FBA1* promoter, used for the strong expression of *XYL2*, was amplified using primer pair pFBA1-U, containing XbaI, and pFBA1-D, containing SphI-XhoI-NotI. The PCR fragment was double digested with XbaI-SphI and cloned into YIp-NH5 to construct YIp-NH6. (vii) *XYL2* from *Scheffersomyces stipitis* was amplified with primer pair XYL2-U, carrying NotI, and XYL2-D, carrying SphI-HpaI-XhoI. The fragment was digested by NotI-SphI and ligated with YIp-NH6 to form YIp-NH7. (viii) The terminator of *FBA1* was amplified using primer pair tFBA1-U and tFBA1-D containing the restriction sites for XhoI and SphI, respectively, and cloned into YIp-NH7, generating plasmid YIp-NH8. The plasmid YIp-NH8 was linearized with restriction endonuclease SpeI prior to being transformed into yeast KAM-XKS1. The resultant strain, carrying the correct integration of *XYL1* and *XYL2* genes, was designated KAM-3X (Table 3).

Plasmid YCplac33 (5) was used to construct pPGK1-noxE for the overexpression of *noxE* driven by the *PGK1* promoter in *S. cerevisiae*. The promoter of *PGK1* was amplified using primer pair pPGK1-U and pPGK1-D (Table 1) containing PstI and SalI, respectively. The PCR fragment was double digested with PstI-SalI and ligated into YCplac33, which had been digested with the same enzyme pair, to construct YCplac33-

TABLE 1 Primers used in this study[a]

Primer name	Sequence	Product or function	Restriction site(s)
pXKS1-U	5′CGGCCAGTGAATTCTGCTTAAGCGGCAGAATTGC3′	pXKS1	EcoRI
pXKS1-D	5′GGGCCCGGTACCGTACTAATCTCATCCTCC3′		KpnI
pTPI1-U	5′GGGCCCGGTACCCCAATGTTCCTAACGGGAGC3′	pTPI1	KpnI
pTPI1-D	5′GGGCCCGGATCCTTTTAGTTTATGTATGTGTT3′		BamHI
XKS1-U	5′CCCGGG GGATCCATGTTGTGTTCAGTAATTC3′	XKS1	BamHI
XKS1-D	5′CCCGGGCTGCAGTTAGATGAGAGTCTTTTCC3′		PstI
XKS1-CKU	5′ATTCCAGTGAATGATCTAC3′	For verification	None
XKS1-CKD	5′CATACAAGGGCATTGTCATG3′		None
NH-1U	5′TACTCCAAGGGTTCGTGACG3′	Homologous fragment	None
NH-1D	5′GGGCCCGGTACCCCAGAATATCTTGGTGAAGC3′		KpnI
NH-2U	5′GGGCCCGCATGCGAGAGCAATCAATGCAATGG3′	Homologous fragment	SphI
NH-2D	5′GGGCCCAAGCTTGGTTGTTCTCAACCTTCTAC3′		HindIII
pHXT7-U	5′GGGCCCGGTACCAGTGGCAGCACGCTAATTCG3′	pHXT7	KpnI
pHXT7-D	5′CGCGCGCCCGGGTTTTTGATTAAAATTAAAAA3′		SmaI
XYL1-U	5′GCGCGCCCCGGGATGCCTTCTATTAAGTTGAAC3′	XYL1	SmaI
XYL1-D	5′GGGCCCTCTAGAGGATCCTTAGACGAAGATAGGAATC3′		XbaI, BamHI
tHXT7-U	5′GGGCCCGGATCCTTTGCGAACACTTTTATTAA3′	tHXT7	BamHI
tHXT7-D	5′GGGCCCGCATGCGCGGCCGCTCTAGACATTAGACACTTTTTGAAGC3′		SphI, NotI, XbaI
pFBA1-U	5′GGGCCCTCTAGACTTCATGCCTCCAACGGCTA3′	pFBA1	XbaI
pFBA1-D	5′GGGCCCGCATGCCTCGAGGCGGCCGCTTTGAATATGTATTACTTGG3′		SphI, XhoI, NotI
XYL2-U	5′GGGCCCGCGGCCGCATGACTGCTAACCCTTCCTTG3′	XYL2	NotI
XYL2-D	5′GGGCCCGCATGCGTTAACCTCGAGTTACTCAGGGCCGTCAATGAG3′		SphI, HpaI, XhoI
tFBA1-U	5′GGGCCCCTCGAGGTTAATTCAAATTAATTGAT3′	tFBA1	XhoI
tFBA1-D	5′GGGCCCGCATGCGGATAAAGTAAGCTACTATG3′		SphI
pPGK1-U	5′CCCGGGCTGCAGAAGAAATTACCGTCGCTCG3′	pPGK1	PstI
pPGK1-D	5′GGGCCCGTCGACAGACATTGTTTTATATTTG3′		SalI
noxE-U	5′GGGCCCGTCGACATGAAAATCGTAGTTATCGG3′	NoxE	SalI
noxE-D	5′GGGCCCGGATCCTTATTTGGCATTCAAAGCTG3′		BamHI
tPGK1-U	5′GGGCCCGGATCCTAAATTGAATTGAATTGAAATC3′	tPGK1	BamHI
tPGK1-D	5′GGGCCCGGTACCGACTTTTTTTGTTGCAAGTGG3′		KpnI

[a] Relevant restriction sites are underlined.

pPGK1. The terminator of *PGK1* was amplified using primer pair tPGK1-U, carrying BamHI, and tPGK1-D, carrying KpnI (Table 1). The resulting fragment was double digested with BamHI and KpnI and inserted into plasmid YCplac33-pPGK1 digested with the same enzyme pair, resulting in plasmid YCplac33-pPGK1-tPGK1. The ORF of the *noxE* gene was amplified from *Lactococcus lactis* genomic DNA (10) using primer pair noxE-U and noxE-D (Table 1), carrying the SalI and BamHI restriction sites, respectively. The PCR fragment was double digested by SalI and BamHI and ligated with YCplac33-pPGK1-tPGK1 digested with the same enzyme pair to form plasmid YCplac33-pPGK1-noxE-tPGK1 (pPGK1-noxE) (Table 2). Plasmids YCplac33 and pPGK1-noxE were transformed into yeast strain KAM-3X for xylose fermentation. The pegylated lithium acetate procedure was used for the transformation of *S. cerevisiae* (33).

TABLE 2 Plasmids constructed and used in this study

Name	Marker and/or description	Source or reference
YCplac33	Amp^r; *URA3*	5
YIplac211	Amp^r; *URA3*	5
pTPI1-XKS1	Amp^r; *URA3*; YIplac211-pXKS1-pTPI1-XKS1	This work
YIp-H8	Amp^r; *URA3*; YIplac211-H1-pHXT7-XYL1-tHXT7-pFBA1-XYL2-tFBA1-H2	This work
pPGK1-noxE	Amp^r; *URA3*; YCplac33-pPGK1-noxE-tPGK1	This work

Preparation of cell extracts and measurement of enzyme activity. Yeast cells (about 2×10^8 cells) for enzyme activity analysis were grown in YSCX medium containing 50 g/liter D-xylose for 12 h, harvested by centrifugation, and washed twice with sterile ice-cold water. The samples for XDH enzyme activity analysis were suspended with 400 μl 0.1 M triethanolamine buffer (pH 7.0) containing 1 mM phenylmethylsulfonyl fluoride, 0.5 mM dithiothreitol, and 0.5 mM EDTA (4). The suspension was disrupted with a FastPrep machine (Thermo Electron) at speed setting 4 for 30 s in the presence of 200 μl glass beads. The samples (about 2×10^8 cells) used for the enzyme activity determination of water-forming NADH oxidase were suspended in 100 mM phosphate buffer (400 μl) containing 2 mM $MgCl_2$ and 1 mM dithiothreitol (29) and were broken with 200 μl glass beads as described above. Cell debris and glass beads from the cell extract were separated by centrifugation at 12,000 rpm for 5 min at 4°C, and the remaining supernatant was used for enzymatic analysis. The concentration of total protein in the supernatant was measured by a Bio-Rad DC protein assay kit using bovine serum albumin as the standard. XDH enzyme activity was determined as previously described (4, 30) using a CECIL 2000 series (Bioquest, England) spectrophotometer at 340 nm. The enzyme activity of water-forming NADH oxidase was measured as micromoles of converted substrate per milligram of protein per minute according to Heux et al. (10).

Xylose fermentation and metabolite analysis. YSCX medium with 50 g/liter D-xylose was used for xylose fermentation. Yeast strains were precultured in YSCD medium containing 20 g/liter glucose for 12 h, and then cells were centrifuged at 12,000 rpm for 2 min. The cell sediments were

TABLE 3 Strains used in this study

Strain	Genotype or description	Source or reference
KAM-2	*MATα ura3*	19
KAM-XKS1	*MATα ura3* pTPI1-XKS1	This work
KAM-3X	*MATα ura3* pHXT7-XYL1-tHXT7 pFBA1-XYL2-tFBA1 pTPI1-XKS1	This work
KAM-3X(YCplac33)	KAM-3X carrying plasmid YCplac33	This work
KAM-3X(pPGK1-NOXE)	KAM-3X carrying plasmid YCplac33-pPGK1-noxE-tPGK1	This work

washed with xylose fermentation medium to remove trace glucose. The xylose fermentation was conducted in 100-ml flasks filled with 40 ml YSCX medium containing 50 g/liter D-xylose. The initial cell density was set to an optical density at 600 nm (OD_{600}) of 1 (corresponding to approximately 0.236 g/liter dry cell mass). In the first 24 h of inoculation, aerobic fermentation was conducted to propagate cells, and then oxygen-limited fermentation was processed. The flask was tightly sealed with parafilm for oxygen-limited fermentation, and a carbon dioxide-releasing channel was created on parafilm with a 0.5-mm injection needle.

Samples were collected every 24 h during the fermentation process and then centrifuged at 12,000 rpm for 5 min. The supernatants were used for chromatographic analysis. Metabolites such as D-xylose, ethanol, glycerol, and organic acid (including acetic acid, succinic acid, and pyruvic acid) were analyzed on a Waters Alliance 2695 high-performance liquid chromatograph (HPLC) (Waters, Milford) using an Aminex HPX 87H column (Bio-Rad) and a Waters 2410 refractive-index detector with a mobile phase of 5 mM H_2SO_4. The flow rate was 0.6 ml/min, and both the column temperature and detection temperature were stabilized at 45°C.

RESULTS

Oxygen-limited batch fermentation of KAM-3X carrying *noxE*. The fermentation details of KAM-3X transformed with plasmid expressing *noxE*, driven by the *PGK1* promoter, were evaluated in oxygen-limited conditions with YSCX medium containing 50 g/liter D-xylose as the sole carbon source. KAM-3X carrying plasmid YCplac33 was used as a reference. Both strains were precultured in YSCD medium containing 20 g/liter glucose to propagate cells. The precultured cells were centrifuged and washed with sterile water to remove trace glucose and resuspended in 40 ml xylose fermentation YSCX medium containing 50 g/liter D-xylose. The initial cell density was about 0.25 g/liter dry cell mass. During the first 24 h after inoculation, aerobic growth was conducted with the fermentation flask covered loosely with aluminum foil. The flask then was tightly sealed with parafilm for oxygen-limited fermentation, and a carbon dioxide channel was created on the film with a 0.5-mm injection needle. Samples were taken out every 24 h for metabolite analysis.

The xylose fermentation details of these two strains are shown in Fig. 2 and Table 4. Under the xylose fermentation conditions with an initial D-xylose concentration of 50 g/liter, KAM-3X(pPGK1-noxE) consumed 44.53 g/liter D-xylose in the medium and the reference strain consumed 47.73 g/liter D-xylose after 120 h fermentation (Fig. 2B). Xylitol formation and yield from D-xylose of KAM-3X carrying *noxE* decreased dramatically, as expected (Fig. 2C and Table 4). The final xylitol concentration and yield of KAM-3X(pPGK1-noxE) were 2.71 g/liter and 0.058 g/g xylose, respectively, while those of the control KAM-3X(YCplac33) were 9.14 g/liter and 0.191 g/g, respectively, which

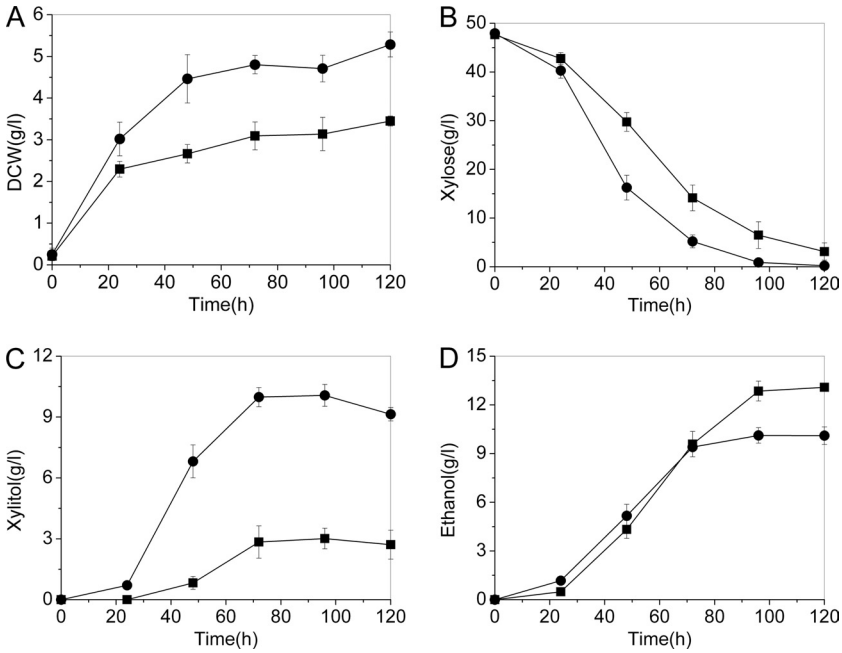

FIG 2 D-Xylose fermentation of KAM-3X(pPGK1-noxE) and KAM-3X(YCplac33) under oxygen-limited conditions in YSCX medium containing 50 g/liter xylose. (A) Biomass concentration; (B) xylose consumption; (C) xylitol formation; (D) ethanol production. Symbols: ■, KAM-3X(pPGK1-noxE); ●, KAM-3X(YCplac33). DCW, dry cell weight.

TABLE 4 The final production of ethanol and yield of biomass, xylitol, ethanol, organic acid, and glycerol at the end of xylose fermentation[a]

Strain	Final ethanol concn (g/liter)	Yield (g [g of xylose consumed]$^{-1}$) of:					Carbon recovery[b]
		Biomass	Xylitol	Ethanol	Organic acid	Glycerol	
KAM-3X(YCplac33)	10.107 ± 0.539	0.112 ± 0.011	0.191 ± 0.010	0.211 ± 0.016	0.014 ± 0.009	0.013 ± 0.001	0.741 ± 0.019
KAM-3X(pPGK1-NOXE)	13.083 ± 0.136	0.071 ± 0.006	0.058 ± 0.029	0.294 ± 0.019	0.037 ± 0.001	0.006 ± 0.003	0.747 ± 0.002

[a] The data are presented as averages and standard deviations from three independent experiments.
[b] Calculated by considering CO_2 production equivalent to ethanol production.

showed a 69.63% decrease of xylitol yield owing to *noxE* overexpression. At the same time, the final ethanol production and yield from D-xylose of KAM-3X(pPGK1-noxE) were 13.083 g/liter and 0.294 g/g, respectively, while those of the control KAM-3X(YCplac33) were 10.107 g/liter and 0.211 g/g, respectively (Fig. 2D and Table 4), which indicated a 39.33% increase due to *noxE* overexpression. Meanwhile, the glycerol yield was reduced by 53.85% owing to the decrease of the NADH pool. However, the organic acid yield was higher than that of the reference (Table 4), and the growth as well as the xylose-consuming rate of KAM-3X(pPGK1-noxE) were inferior to those of the control KAM-3X(YCplac33) (Fig. 2A and B). The slow growth and xylose consumption rates probably were caused by the overexpression of *noxE*, which might lead to redox imbalance, hence affecting cell growth (10). To clarify this phenomenon, the enzyme activities of NADH oxidase and XDH were measured to see if the microcycle we are trying to build was in balance.

The enzyme activity of NADH oxidase and XDH. Cells for the enzyme activity analysis of NADH oxidase and XDH in KAM-3X(pPGK1-noxE) and the control KAM-3X(YCplac33) were cultured in YSCX medium containing 50 g/liter D-xylose. Cells were harvested after aerobic growth for 12 h; the preparation of samples and the enzymatic analysis procedure are described in Materials and Methods. The enzymatic analysis of the crude extracts from KAM-3X(pPGK1-noxE) showed NADH oxidase activity of 1.13 ± 0.03 U/mg and XDH activity of 0.59 ± 0.02 U/mg. The activity of XDH in the control strain was 0.56 ± 0.04 U/mg, and basal NADH dehydrogenase activity was not detected. The enzymatic activity of NADH oxidase was a little higher than XDH activity in the same strain, which indicated that the microcycle between NADH and NAD^+ was not in a completely balanced situation according to the enzymatic data.

DISCUSSION

We have expressed the *Lactococcus lactis noxE* gene, encoding a water-forming NADH oxidase, in the xylose-utilizing *S. cerevisiae* strain KAM-3X under the control of the *PGK1* promoter, which resulted in a 69.63% decrease in xylitol yield and a 39.33% increase in ethanol yield. This result indicates for the first time that the constitution of a microcycle of NAD^+ consumption, catalyzed by XDH, and regeneration caused by *noxE* is an effective strategy to deal with the problem of redox imbalance in a xylose-utilizing *S. cerevisiae* strain. In theory, other cellular processes coupled with cofactor NADH and NAD^+, such as glycerol synthesis and organic acid formation, also could be affected (Fig. 1). Consistently with this notion, we observed a decrease in glycerol production (53.85%), which may contribute partially to the increased ethanol yield and an increase in organic acid formation (Table 4). This also is consistent with the results of previous studies (10, 34). Apparently, the imbalance between the activity of the NADH oxidase for NADH (1.13 U/mg) and that of XDH for NAD^+ (0.59 U/mg) led to the overoxidization of NADH and hence affected the metabolic processes in which NADH and NAD^+ participated. As a consequence, the growth rate and xylose consumption of KAM-3X carrying *noxE* was affected as reported previously (10, 34).

To overcome the redox cofactor imbalance in the xylose metabolic pathway, some efforts were made to manipulate or introduce other pathways involved in cofactor metabolism (3, 6, 13, 36). Shifting ammonia assimilation from an NADPH- to NADH-dependent process by the deletion of *gdh1* and the overexpression of *GDH2* resulted in a 16% higher ethanol yield and 44% less xylitol excretion (6). The simultaneous overexpression of the fungal *GDP1* gene and the deletion of *zwf1* enhanced the rate and yield of ethanol production and lowered xylitol accumulation (36). The expression of the *Streptococcus mutans gapN* gene in a xylose-utilizing yeast strain reduced the formation of glycerol and xylitol by 58 and 33%, respectively, while it increased the production of ethanol by 24% (3). Engineering a cofactor preference for XR and/or XDH to address the problem of xylitol formation produced positive results with limited satisfaction (12, 27, 28, 38, 40). In the present study, the *noxE*-expressing recombinant strain produced 29.45% more ethanol and 70.35% less xylitol than the reference strain. The 70.35% decrease of xylitol is by far the optimal result.

Further work could focus on fine-turning the promoter strength of *noxE* and *XYL2* to balance the cellular activity of the two enzymes. In addition, establishing a microcycle between the oxidation of NADPH by XR and the regeneration of NADPH by *GDP1* (36) or *gapN* (3), like the *noxE*-XDH cycle in our recombinant strain, would be helpful for efficient xylose utilization. However, xylitol production during xylose fermentation is a complex phenomenon and cannot be eliminated by merely balancing the cofactors, and since cofactor imbalance is not the only parameter governing ethanolic xylose fermentation, more work needs to be done in this field.

ACKNOWLEDGMENTS

We express our deepest appreciation to our Ph.D. promoter, P. Ma, for his valuable instruction and constructive advice on the study which formed the basis of this paper.

We are grateful for financial support from the Innovation Foundation of Tianjin University.

REFERENCES

1. **Ansell R, Granath K, Hohmann S, Thevelein JM, Adler L.** 1997. The two isoenzymes for yeast NAD+-dependent glycerol 3-phosphate dehydrogenase encoded by *GPD1* and *GPD2* have distinct roles in osmoadaptation and redox regulation. EMBO J. **16**:2179–2187.
2. **Brat D, Boles E, Wiedemann B.** 2009. Functional expression of a bacterial xylose isomerase in *Saccharomyces cerevisiae.* Appl. Environ. Microbiol. **75**:2304–2311.
3. **Bro C, Regenberg B, Forster J, Nielsen J.** 2006. In silico aided metabolic

engineering of *Saccharomyces cerevisiae* for improved bioethanol production. Metab. Eng. **8**:102–111.
4. **Eliasson A, Christensson C, Wahlbom CF, Hahn-Hagerdal B.** 2000. Anaerobic xylose fermentation by recombinant *Saccharomyces cerevisiae* carrying *XYL1*, *XYL2*, and *XKS1* in mineral medium chemostat cultures. Appl. Environ. Microbiol. **66**:3381–3386.
5. **Gietz RD, Sugino A.** 1988. New yeast-Escherichia coli shuttle vectors constructed with in vitro mutagenized yeast genes lacking six-base pair restriction sites. Gene **74**:527–534.
6. **Grotkjaer T, Christakopoulos P, Nielsen J, Olsson L.** 2005. Comparative metabolic network analysis of two xylose fermenting recombinant *Saccharomyces cerevisiae* strains. Metab. Eng. **7**:437–444.
7. **Hahn-Hägerdal B, Karhumaa K, Fonseca C, Spencer-Martins I, Gorwa-Grauslund MF.** 2007. Towards industrial pentose-fermenting yeast strains. Appl. Microbiol. Biotechnol. **74**:937–953.
8. **Hahn-Hägerdal B, Karhumaa K, Jeppsson M, Gorwa-Grauslund MF.** 2007. Metabolic engineering for pentose utilization in *Saccharomyces cerevisiae.* Adv. Biochem. Eng. Biotechnol. **108**:147–177.
9. **Harhangi HR, et al.** 2003. Xylose metabolism in the anaerobic fungus *Piromyces* sp. strain E2 follows the bacterial pathway. Arch. Microbiol. **180**:134–141.
10. **Heux S, Cachon R, Dequin S.** 2006. Cofactor engineering in *Saccharomyces cerevisiae*: expression of a H_2O-forming NADH oxidase and impact on redox metabolism. Metab. Eng. **8**:303–314.
11. **Hoefnagel MH, et al.** 2002. Metabolic engineering of lactic acid bacteria, the combined approach: kinetic modelling, metabolic control and experimental analysis. Microbiology **148**:1003–1013.
12. **Hou J, Shen Y, Li XP, Bao XM.** 2007. Effect of the reversal of coenzyme specificity by expression of mutated *Pichia stipitis* xylitol dehydrogenase in recombinant *Saccharomyces cerevisiae.* Lett. Appl. Microbiol. **45**:184–189.
13. **Hou J, Vemuri GN, Bao X, Olsson L.** 2009. Impact of overexpressing NADH kinase on glucose and xylose metabolism in recombinant xylose-utilizing *Saccharomyces cerevisiae.* Appl. Microbiol. Biotechnol. **82**:909–919.
14. **Jeffries TW.** 2006. Engineering yeasts for xylose metabolism. Curr. Opin. Biotechnol. **17**:320–326.
15. **Jeppsson M, et al.** 2006. The expression of a *Pichia stipitis* xylose reductase mutant with higher K(M) for NADPH increases ethanol production from xylose in recombinant *Saccharomyces cerevisiae.* Biotechnol. Bioeng. **93**:665–673.
16. **Jin YS, Jeffries TW.** 2003. Changing flux of xylose metabolites by altering expression of xylose reductase and xylitol dehydrogenase in recombinant *Saccharomyces cerevisiae.* Appl. Biochem. Biotechnol. **105–108**:277–286.
17. **Karhumaa K, Fromanger R, Hahn-Hagerdal B, Gorwa-Grauslund MF.** 2007. High activity of xylose reductase and xylitol dehydrogenase improves xylose fermentation by recombinant *Saccharomyces cerevisiae.* Appl. Microbiol. Biotechnol. **73**:1039–1046.
18. **Karhumaa K, Garcia Sanchez R, Hahn-Hagerdal B, Gorwa-Grauslund MF.** 2007. Comparison of the xylose reductase-xylitol dehydrogenase and the xylose isomerase pathways for xylose fermentation by recombinant *Saccharomyces cerevisiae.* Microb. Cell Fact. **6**:5.
19. **Kong QX, et al.** 2006. Improved production of ethanol by deleting *FPS1* and over-expressing GLT1 in *Saccharomyces cerevisiae.* Biotechnol. Lett. **28**:2033–2038.
20. **Kurtzman CP, Suzuki M.** 2010. Phylogenetic analysis of ascomycete yeasts that form coenzyme Q.-9 and the proposal of the new genera *Babjeviella*, *Meyerozyma*, *Millerozyma*, *Priceomyces*, and *Scheffersomyces.* Mycoscience **51**:2–14.
21. **Kuyper M, et al.** 2003. High-level functional expression of a fungal xylose isomerase: the key to efficient ethanolic fermentation of xylose by *Saccharomyces cerevisiae*? FEMS Yeast Res. **4**:69–78.
22. **Liang L, Zhang J, Lin Z.** 2007. Altering coenzyme specificity of *Pichia stipitis* xylose reductase by the semi-rational approach CASTing. Microb. Cell Fact. **6**:36.
23. **Liu EK, Hu Y.** 2010. Construction of a xylose-fermenting *Saccharomyces cerevisiae* strain by combined approaches of genetic engineering, chemical mutagenesis and evolutionary adaptation. Biochem. Eng. J. **48**:204–210.
24. **Lopez de Felipe F, Kleerebezem M, de Vos WM, Hugenholtz J.** 1998. Cofactor engineering: a novel approach to metabolic engineering in *Lactococcus lactis* by controlled expression of NADH oxidase. J. Bacteriol. **180**:3804–3808.
25. **Madhavan A, et al.** 2009. Xylose isomerase from polycentric fungus *Orpinomyces*: gene sequencing, cloning, and expression in *Saccharomyces cerevisiae* for bioconversion of xylose to ethanol. Appl. Microbiol. Biotechnol. **82**:1067–1078.
26. **Matsushika A, Inoue H, Kodaki T, Sawayama S.** 2009. Ethanol production from xylose in engineered *Saccharomyces cerevisiae* strains: current state and perspectives. Appl. Microbiol. Biotechnol. **84**:37–53.
27. **Matsushika A, et al.** 2008. Expression of protein engineered NADP+-dependent xylitol dehydrogenase increases ethanol production from xylose in recombinant *Saccharomyces cerevisiae.* Appl. Microbiol. Biotechnol. **81**:243–255.
28. **Petschacher B, Nidetzky B.** 2008. Altering the coenzyme preference of xylose reductase to favor utilization of NADH enhances ethanol yield from xylose in a metabolically engineered strain of *Saccharomyces cerevisiae.* Microb. Cell Fact. **7**:9.
29. **Remize F, Andrieu E, Dequin S.** 2000. Engineering of the pyruvate dehydrogenase bypass in *Saccharomyces cerevisiae*: role of the cytosolic Mg(2+) and mitochondrial K(+) acetaldehyde dehydrogenases Ald6p and Ald4p in acetate formation during alcoholic fermentation. Appl. Environ. Microbiol. **66**:3151–3159.
30. **Rizzi M, Harwart K, Erlemann P, Bui-Thanh N-A, Dellweg H.** 1989. Purification and properties of the NAD+-xylitol-dehydrogenase from the yeast *Pichia stipitis.* J. Ferment. Bioeng. **67**:20–24.
31. **Rodriguez-Peña JM, Cid VJ, Arroyo J, Nombela C.** 1998. The YGR194c (XKS1) gene encodes the xylulokinase from the budding yeast *Saccharomyces cerevisiae.* FEMS Microbiol. Lett. **162**:155–160.
32. **Runquist D, Hahn-Hagerdal B, Bettiga M.** 2010. Increased ethanol productivity in xylose-utilizing *Saccharomyces cerevisiae* via a randomly mutagenized xylose reductase. Appl. Environ. Microbiol. **76**:7796–7802.
33. **Schiestl RH, Gietz RD.** 1989. High efficiency transformation of intact yeast cells using single stranded nucleic acids as a carrier. Curr. Genet. **16**:339–346.
34. **Vemuri GN, Eiteman MA, McEwen JE, Olsson L, Nielsen J.** 2007. Increasing NADH oxidation reduces overflow metabolism in *Saccharomyces cerevisiae.* Proc. Natl. Acad. Sci. U. S. A. **104**:2402–2407.
35. **Verduyn C, et al.** 1985. Properties of the NAD(P)H-dependent xylose reductase from the xylose-fermenting yeast *Pichia stipitis.* Biochem. J. **226**:669–677.
36. **Verho R, Londesborough J, Penttila M, Richard P.** 2003. Engineering redox cofactor regeneration for improved pentose fermentation in *Saccharomyces cerevisiae.* Appl. Environ. Microbiol. **69**:5892–5897.
37. **Walfridsson M, et al.** 1996. Ethanolic fermentation of xylose with *Saccharomyces cerevisiae* harboring the *Thermus thermophilus xylA* gene, which expresses an active xylose (glucose) isomerase. Appl. Environ. Microbiol. **62**:4648–4651.
38. **Watanabe S, et al.** 2007. Ethanol production from xylose by recombinant *Saccharomyces cerevisiae* expressing protein-engineered NADH-preferring xylose reductase from *Pichia stipitis.* Microbiology **153**:3044–3054.
39. **Watanabe S, Kodaki T, Makino K.** 2005. Complete reversal of coenzyme specificity of xylitol dehydrogenase and increase of thermostability by the introduction of structural zinc. J. Biol. Chem. **280**:10340–10349.
40. **Watanabe S, et al.** 2007. The positive effect of the decreased NADPH-preferring activity of xylose reductase from *Pichia stipitis* on ethanol production using xylose-fermenting recombinant *Saccharomyces cerevisiae.* Biosci. Biotechnol. Biochem. **71**:1365–1369.